Nutrient-dependent regulation of β-cell K_{ATP} channels is locally controlled by the isoforms of pyruvate kinase and the source of phosphoenolpyruvate

Hannah R. Foster[1], Thuong Ho[1], Evgeniy Potapenko[1], Sophia M. Sdao[1], Sophie L. Lewandowski[1], Halena R. VanDeusen[1], Shawn M. Davidson[2,3], Rebecca L. Cardone[4], Richard G. Kibbey[4,5], and Matthew J. Merrins[1,6*]

[1]Department of Medicine, Division of Endocrinology, Diabetes, and Metabolism, University of Wisconsin-Madison, Madison, WI, USA
[2]Koch Institute for Integrative Cancer Research, Massachusetts Institute of Technology, Cambridge, MA, USA
[3]Lewis-Sigler Institute for Integrative Genomics, Princeton University, Princeton, NJ, USA
[4]Department of Internal Medicine, Yale University, New Haven, CT, USA
[5]Department of Cellular & Molecular Physiology, Yale University, New Haven, CT, USA
[6]William S. Middleton Memorial Veterans Hospital, Madison, WI, USA
*Correspondence: mmerrins@medicine.wisc.edu

SUMMARY

Pancreatic β-cells use phosphoenolpyruvate (PEP) cycling by pyruvate kinase (PK) to signal appropriate insulin secretion. Here, we show that the isoforms of PK, together with the PEP generated by mitochondrial PEP carboxykinase (PCK2), endow ATP-sensitive K^+ (K_{ATP}) channels with nutrient sensitivity and specificity. Glucose-dependent regulation of the K_{ATP} channel is locally controlled by the allosterically tunable PKm2 isoform, which is remarkable considering that PKm1 accounts for >90% of cellular activity and is sufficient for K_{ATP} closure in the channel microcompartment. Mitochondrial signaling to the plasma membrane, which determines the β-cell response to amino acids, depends on both PCK2 and PKm1 to close K_{ATP} channels. In addition to these membrane depolarizing "on-switches," we identified a mitochondrial PEP-dependent "off-switch" that regulates the length of depolarization. This back and forth communication between the K_{ATP} channel and mitochondria via highly compartmentalized PEP metabolism controls the oscillatory cycle regulating insulin secretion.

KEYWORDS

Pyruvate kinase, phosphoenolpyruvate, PKm1, PKm2, PCK2, K_{ATP} channels, β-cell metabolism, PEP cycle, ATP/ADP, Ca^{2+} oscillations, insulin secretion

INTRODUCTION

Maintenance of euglycemia relies on β-cells to couple nutrient sensing with appropriate insulin secretion. Plasma membrane-localized pyruvate kinase (PK) plays a key role in this nutrient response by converting phosphoenolpyruvate (PEP) and ADP to pyruvate and ATP, locally raising the ATP/ADP ratio in the K_{ATP} channel microcompartment to depolarize the membrane and initiate insulin secretion[1]. This local mechanism of control obviates the "standard model" of β-cell fuel sensing in which mitochondrial oxidative phosphorylation raises the ATP/ADP ratio to close K_{ATP} channels[2–4]—a concept that conflicts with the thermodynamic principle of mitochondrial respiratory control[1,5,6]. As such, Lewandowski *et al.*[1] recently proposed a revised model of β-cell fuel sensing, which we refer to here as the $Mito_{Cat}$-$Mito_{Ox}$ model, that is relevant to human islets and the *in vivo* context[1,7].

In this oscillatory model of β-cell metabolism, ADP availability dictates the metabolic cycles that preferentially occur during the electrically-silent triggering phase or the electrically-active secretory phase of glucose-stimulated oscillations (**Fig. S1**). During the triggering phase, the favorable bioenergetics of PK-driven PEP hydrolysis progressively lowers ADP and slows oxidative phosphorylation, precluding mitochondria from generating ATP/ADP near K_{ATP} in a phase of metabolism termed $Mito_{Cat}$ (a.k.a. $Mito_{Synth}$[1]). The shift to a higher $\Delta\Psi_m$ and ATP/ADP ratio elevates the NADH/NAD^+ ratio in the mitochondrial matrix and stalls the TCA cycle. The ensuing increase in acetyl-CoA allosterically activates pyruvate carboxylase, the anaplerotic consumer of pyruvate that fuels oxaloacetate-dependent PEP cataplerosis by mitochondrial PEP carboxykinase (PCK2). The return of mitochondrial PEP to the cytosol completes the "PEP cycle" that augments ATP/ADP generation by cytosolic PK, which locally closes K_{ATP} channels. Following membrane depolarization, the increased workload (ATP hydrolysis) associated with Ca^{2+} extrusion and exocytosis elevates ADP, which activates oxidative phosphorylation to sustain the secretory phase in a phase referred to as $Mito_{Ox}$.

In the $Mito_{Cat}$-$Mito_{Ox}$ model, PK has two possible sources of PEP that may differentially regulate K_{ATP} closure: glycolytic PEP produced by enolase, and mitochondrial PEP produced by PCK2 in response to anaplerosis (**Fig. 1a**). About 40% of glucose-derived PEP is generated by PCK2 in the PEP cycle and closely linked to insulin secretion[7–9], suggesting a role in glucose-stimulated oscillations. Mitochondrial PEP derived from PCK2 may also provide a glycolysis-independent mechanism by which PK rapidly increases the cytosolic ATP/ADP ratio locally at the K_{ATP} channel in response to amino acids, which are potent anaplerotic fuels.

The isoforms of PK, each with different activities and mechanisms of control, may also be important regulators of K_{ATP} channel closure (**Fig. 1a**). β-cells express the constitutively-active PKm1 as well as two allosterically-recruitable isoforms, PKm2 and PKL, which are activated by glycolytic fructose-1,6-bisphosphate (FBP) generated upstream by the phosphofructokinase-1 reaction[10–12]. Pharmacologic PK activators (PKa), which lower the K_m of PKm2 for PEP and increase V_{max}[13], increase the frequency of glucose-stimulated Ca^{2+} and ATP/ADP oscillations and potentiate nutrient-stimulated insulin secretion from rodent and human islets[1,7]. Much less is known about the PKm1 isoform, whose constitutive activity may be ideal in situations of high

oxidative workload, as in cardiac myocytes[14]. β-cells may shift their reliance upon different PK isoforms throughout the oscillatory cycle, as the levels of glycolytic FBP rise during $Mito_{Cat}$ and fall during $Mito_{Ox}$[1,15,16].

Here, we demonstrate that both PKm1 and PKm2 are active in the K_{ATP} channel microcompartment with at least two essential functions. First, shared control over K_{ATP} closure provides redundancy in the β-cell response to glucose. Such spatial privilege permits the minor PKm2 isoform, when activated by FBP, to transmit the signal from glucose to K_{ATP} despite contributing a small fraction of the whole cell PK activity. Second, the composition of PK isoforms within the compartment tunes the β-cell response to mitochondrial fuels such as amino acids, which provide mitochondrial PEP without also generating the FBP needed to allosterically activate PKm2. β-cell PCK2, in the mitochondria, signals to the plasma membrane K_{ATP} microcompartment during $Mito_{Cat}$ and is essential for cytosolic ATP/ADP generation. In addition, PCK2 signals via PKm2 to facilitate Ca^{2+} extrusion during $Mito_{Ox}$. These data augment the $Mito_{Cat}$-$Mito_{Ox}$ model of oscillatory β-cell metabolism by identifying unique roles for the PKm1- and PKm2-driven PEP cycles in nutrient sensing.

RESULTS

PKm1 accounts for >90% of β-cell PK activity with only a small contribution from PKm2

We generated β-cell specific PKm1 and PKm2 knockout mice by breeding *Ins1-Cre* mice[17] with *Pkm1*$^{f/f}$ mice[14,18] (PKm1-βKO) or *Pkm2*$^{f/f}$ mice[19] (PKm2-βKO). PKm1 protein was reduced by 71% in PKm1-βKO islets, while PKm2 increased by 46% compared to littermate *Ins1-Cre* controls (**Fig. 1b**). Comparatively, expression of PKm2 protein fell by 94% in PKm2-βKO islets, while PKm1 increased by 29% (**Fig. 1c**). In both strains this partial compensation is expected since PKm1 and PKm2 are alternative splice variants of the *Pkm* gene[14,19]. *Pck2*$^{f/f}$ mice were generated *de novo* (**Fig. S2**) and crossed with *Ucn3-Cre* mice to facilitate postnatal β-cell deletion without the need for tamoxifen[20]. Islet PCK2 protein dropped by 67% in the Pck2-βKO compared to Pck2-floxed littermate controls (**Fig. 1d**). None of these knockout mice were glucose intolerant (**Fig. 1e-g**).

The relative contributions of each PK isoform relative to total PK activity was determined in the islet lysates. The endogenous allosteric metabolite, FBP, and pharmacologic PK activators such as TEPP-46 (PKa), have no impact on PKm1 but substantially lower the K_m and raise V_{max} for PKm2 or PKL[1]. Control islet lysates had a K_m for PEP of ~140 ± 14 μM that did not change significantly in the presence of exogenous FBP (K_m, 100 μM ± 10 μM) or PKa (K_m, 90 ± 13 μM), while V_{max} increased by about one-third (control, 1.05 ± 0.019 μmol/min; FBP, 1.28 ± 0.006 μmol/min; PKa, 1.36 ± 0.006 μmol/min). Quite remarkably the V_{max} for islet PK activity from PKm1-βKO mice was reduced by 97% compared to controls (**Fig. 1h**), and was too low to estimate K_m accurately. The residual PK remained sensitive to activation by both FBP and PKa and identified a recruitable pool that accounted for only about 10% of the PK activity present in controls islets (**Fig. 1h**), despite compensation from elevated PKm2 protein (**Fig. 1b**). Conversely,

β-cell PKm2 deletion lowered islet lysate PK V_{max} by ~20% in the absence of activators, and eliminated both the K_m and V_{max} response to PKa and FBP (**Fig. 1i**), thus ruling out any significant PKL activity. Taken together, mouse islet PK activity is composed of >90% PKm1, with a variable contribution from PKm2 depending on the FBP level, and no discernable contribution from PKL. Given that PKm1 has a low K_m, if only considered in terms of total cellular activity (*i.e.* in the absence of any compartmentalized functions), PKm1 should be dominant over PKm2 under all physiologic conditions but especially when the PEP concentration is low.

PKm1 is sufficient for K_{ATP} channel closure in the plasma membrane microcompartment, while PKm2 must be allosterically activated

We previously demonstrated that PK, by virtue of its colocalization with K_{ATP} channels, generates a sufficient ATP/ADP ratio to close the channels in mouse and human β-cells even under saturating ADP[1]. These excised patch-clamp experiments, which expose the inside of the plasma membrane to the bath solution (*i.e.* the inside-out mode), provide both the location of PK as well as its functional coupling to K_{ATP} channels in native β-cell membranes. This approach was re-applied in combination with β-cell deletion of PKm1 and PKm2 to identify the isoforms present in the K_{ATP} microdomain. K_{ATP} channels were identified by inhibition with 1 mM ATP, which blocked the spontaneous opening that occurs after patch excision (**Fig. 2a**). Channel activity was restored using a test solution containing 0.5 mM ADP. In control β-cells, the further addition of 5 mM PEP reduced the total power (a term reflecting both the frequency and channel open time) by 77% in control β-cells (**Fig. 2a**), compared with only a 29% reduction in PKm1-βKO cells (**Fig. 2b**). Note that K_{ATP} channel closure occurred in control β-cells despite the continuous deluge of the channel-opener ADP, which must therefore be locally depleted for K_{ATP} channels to close, placing PK in the K_{ATP} channel microcompartment. Thus, it is not the PEP *per se* but the PK activity in the K_{ATP} microcompartment that is responsible for K_{ATP} closure.

To test for PKm2 in the K_{ATP} microcompartment, PKm1-βKO cells were preincubated in presence of 10 μM PKa, which together with PEP restored K_{ATP} channel closure to control levels with 1 mM ATP alone (**Fig. 2c**). PKa had a similar effect when applied acutely (**Fig. 2d**), indicating that PKm2 does not require allosteric activation to localize to the K_{ATP} microdomain. In addition, since the PEP concentration in the incubations were well over the K_m of either isoform, the response to PKa indicates that channel closure either requires an additional increase in the V_{max} or that the functional interaction is sensitive to the quaternary structure of PKm2 (**Fig. 2c-d**). β-cells lacking PKm2 maintained channel closure without PKa with the same power as 1 mM ATP, which is attributable to the sufficiency of endogenous PKm1 (**Fig. 2e**). Metabolic compartmentation of PKm1 and PKm2 provides enzymatic redundancy as well as a compelling explanation for the ability of PKm1-βKO mice to tolerate a near complete loss of PK activity (**Fig. 1e,h**).

PKm2 and mitochondrial PEP, but not PKm1, have metabolic control over glucose-stimulated Ca^{2+} oscillations

The rescue of PKm1 deficiency by PKa in the K_{ATP} microcompartment suggests that PKm1 and PKm2 share local metabolic control over K_{ATP} closure, provided that glucose is available to

generate the FBP needed to activate PKm2 (**Fig. 2c-d**). To test this further we examined Ca^{2+} dynamics with FuraRed while using a near-IR dye, DiR, to facilitate simultaneous imaging of PKm1-, PKm2-, and PCK2-βKO islets with their littermate controls (**Fig. 3a**). Indeed, β-cell deletion of PKm1 or PKm2 did not reveal any biologically meaningful differences in the oscillatory period, the fraction of each oscillation spent in the electrically-active state (*i.e.* the duty cycle), or amplitude of glucose-stimulated Ca^{2+} oscillations in intact islets (**Fig. 3b-c**) confirming *in situ* that they are redundant at high glucose. Importantly, the observation that steady-state Ca^{2+} oscillations are normal in PKm1-βKO islets, which retain at maximum only ~10% of PK activity (**Fig. 1h**), indicates that remarkably PK is not kinetically limited (*i.e.* by V_{max}) in either the cataplerotic ($Mito_{Cat}$) or oxidative phases ($Mito_{Ox}$) of the oscillation (**Fig. 3a**). It is especially notable then, that the acute application of PKa to normal islets reduced the period as well as the amplitude of the steady-state glucose-induced oscillations (**Fig. 3d and Fig. S3a**), indicating significant control by PKm2.

Increasing the glucose concentration will reduce the time spent in the electrically-silent $Mito_{Cat}$ phase of the oscillations (**Fig. S3b**) by accelerating PK-dependent K_{ATP} closure (**Fig. 2d**), while dramatically increasing the fraction of the time spent in the electrically-active $Mito_{Ox}$ phase of the oscillation (i.e. the duty cycle), thereby increasing the oscillatory period[1]. Interestingly, PKa shortened *both* $Mito_{Cat}$ and $Mito_{Ox}$ to similar extents (**Fig. S3c**) effectively preserving the duty cycle while reducing the period (**Fig. 3d**). These striking observations suggest that, unlike glucose elevation, the PK-driven PEP cycle regulates the onset *and* termination of Ca^{2+} influx. Conversely, in PCK2-βKO islets, both the period and amplitude of glucose-stimulated Ca^{2+} oscillations were increased relative to controls islets (**Fig. 3e**). The period lengthening occurred from increased durations of *both* $Mito_{Cat}$ and $Mito_{Ox}$ (**Fig. S3d**) and though the duty cycle increased significantly, it was only by a small fraction. This indicates that at a fixed glucose concentration, the "on" and "off" switches arising from PKm2 activation are balanced, and they are substrate-limited by mitochondrial production of PEP.

The above experiments examined conditions at a fixed glucose concentration that may not relate to the transition from low to high glucose where first-phase secretion is observed. Following an acute rise from 2 to 10 mM glucose, PKm1 and PKm2 knockouts had no discernable difference in first-phase Ca^{2+} parameters (i.e., time to depolarization, amplitude, and duration of first phase) (**Fig. 3f-g**). In contrast, addition of PKa to control islets reduced the time to depolarization as well as the duration of the first-phase (**Fig. 3h**). Conversely, depolarization was delayed in Pck2-βKO islets (**Fig. 3i**). However, in this case the duration of the first-phase Ca^{2+} pulse was not calculated since nearly 60% of Pck2-βKO islets failed to exit the first phase plateau in order to begin oscillations, as compared with only 20% of control islets (**Fig. 3i**). That is, while PCK2 knockout had a weaker first phase Ca^{2+} rise, it had a much longer plateau that failed to turn off effectively. So, like the steady-state, PKm2 activation and PCK2 metabolism control Ca^{2+}, both serving as on-switches during the triggering phase, $Mito_{Cat}$, and off-switches during the secretory phase, $Mito_{Ox}$.

Restriction of glycolytic PEP reveals the importance of PCK2 for cytosolic ATP/ADP

Amino acids (AA) are obligate mitochondrial fuels that simultaneously feed oxidative and anaplerotic pathways. Independent of glycolysis, they generate PEP via glutamate dehydrogenase (GDH)-mediated anaplerosis that is followed by PCK2-mediated cataplerosis via the mitochondrial GTP cycle[8,21]. AA are a tool for separating mechanistic components of the secretion mechanism because at low glucose they raise ATP/ADP but only elicit a single wave of K_{ATP} channel closure, Ca^{2+}, and insulin release. We used β-cell specific expression of Perceval-HR biosensors to examine whether restriction of the mitochondrial PEP supply (via Pck2-βKO knockout) impacted the cytosolic ATP/ADP ratio[22,23]. To limit glycolytic PEP, islets in 2.5 mM glucose were stimulated with a mixture of AA including leucine and glutamine to allosterically activate and fuel GDH, respectively. Consistent with defective PEP cataplerosis, the ATP/ADP response of PCK2-βKO islets was only 37% of control islets in response to AA (**Fig. 4a**) suggesting that the majority of the ATP/ADP increase was PCK2 dependent. In this setting of PCK2 depletion, PK activation did not recover any of the ATP/ADP response (**Fig. 4b)** as expected from the absence of a glycolytic PEP source. Deletion of either PKm1 or PKm2 modestly reduced the β-cell ATP/ADP response to AA (**Fig. 4c,e**), indicating a redundancy for raising ATP/ADP in the absence of glycolytic FBP or PEP. Akin to the patch-clamp studies in **Fig. 2c-d**, PKa completely recovered the PKm1-βKO islets but not the PKm2-βKO islets (**Fig. 4d,f**), indicating that the PKm2 isoform is required for maximal ATP/ADP ratios from AA and that PKm2 is also sufficient in the absence of PKm1. Thus, both PK isoforms redundantly increase the cytosolic ATP/ADP ratio via the PEP cycle. In contrast, PCK2 is essential for amino acids and displays high control strength over ATP/ADP considering that the protein was only reduced by about two-thirds (**Fig. 1d**).

Mitochondrial PEP drives K_{ATP} closure and Ca^{2+} influx during $Mito_{Cat}$, while accelerating K_{ATP} reopening and Ca^{2+} extrusion during $Mito_{Ox}$

Mitochondria are located throughout the β-cell, including near the plasma membrane[24,25]. To determine whether cytosolic ATP/ADP generated via PK from mitochondrial PEP impacts the K_{ATP} channel microcompartment, we monitored K_{ATP} channel currents in *intact* β-cells in the cell-attached configuration in response to bath-applied AA at low glucose (**Fig. 5a**). Mixed AA with or without PKa reduced K_{ATP} channel power (reflecting the total number of transported K^+ ions) by ~75% in control β-cells, while the further addition of PKa after K_{ATP} closure (during $Mito_{Ox}$) partially reopened the channel (**Fig. 5b**). The channel opening with PKa suggests that PKm2 activation also controls a functionally separable "off" switch that ultimately increases the channel excitability from mitochondrial PEP, which was necessary to switch off Ca^{2+} influx (**Fig. 3e,i**). In other words, PKm2 may switch from an activating function during $Mito_{Cat}$ to an inactivating function during $Mito_{Ox}$, consistent with the ability of PKa to both hasten the onset *and* shorten the duration of Ca^{2+} pulses (**Fig. 3d,h**).

As in excised patches (**Fig. 2b**), β-cells from the PKm1-βKO islets failed to respond to mitochondrial PEP (**Fig. 5c**), indicating that PKm2 requires allosteric recruitment in the absence of glycolytic FBP. Islets preincubated with PKa demonstrated K_{ATP} channel closing by AA (**Fig. 5d**), resembling the control islets (**Fig. 5b**). β-cells from the PKm2-βKO mice remained sensitive

to AA-stimulated K_{ATP} closure (**Fig. 5e**) as in the excised patch experiments (**Fig. 2e**). No K_{ATP} closure was observed in the absence of PCK2, even with activator present, demonstrating the essentiality of mitochondrial PEP for AA-stimulated K_{ATP} closure, and confirming that the mitochondrial anaplerotic/cataplerotic pathway had been isolated from glycolysis with this technique (**Fig. 5f**). Taken together, these data reveal that mitochondrial PEP generated in response to AA is capable of locally signaling to PK in the K_{ATP} channel microcompartment through PKm1 or activated PKm2 in an intact islet β-cell.

While AA-stimulated K_{ATP} closure does not induce multiple Ca^{2+} oscillations as glucose does, Ca^{2+} influx follows a distinct triggering and recovery phase, representing $Mito_{Cat}$ and $Mito_{Ox}$, respectively (**Fig. 5g**). Mechanistically, the on-switch function of allosterically activated PKm2 is specific to $Mito_{Cat}$, whereas during $Mito_{Ox,}$ when Ca^{2+} is actively being lowered by ATPases, PK can act as an off-switch that helps reopen K_{ATP} to reset the system (**Fig. 5c**). To test this concept further, we examined the effect of PKa on AA-stimulated Ca^{2+} influx. When applied early during $Mito_{Cat}$, PKa increased AA-stimulated Ca^{2+} influx (**Fig. 5h**), while PKa application during $Mito_{Ox}$ reduced cytosolic Ca^{2+} (**Fig. 5i**), confirming two temporally separated functions of PKm2 in response to mitochondrial PEP.

The isoforms of PK, and the source of PEP, dictate the Ca^{2+} and insulin secretory response to anaplerotic fuels

We next examined the functional consequence of β-cell PKm1, PKm2, and PCK2 deletion on AA-stimulated Ca^{2+} influx and insulin secretion at both low and high glucose (**Fig. 6**). In intact PCK2-βKO islets at low glucose, like the ATP/ADP ratio (**Fig. 4a**), the AA-induced Ca^{2+} response was reduced along with insulin secretion (**Fig. 6a,b**). Thus, compared to controls, there is a substrate-limited dependency on PCK2 to generate sufficient PEP that is needed to fully engage the secretory apparatus. This dependency on PCK2 was not apparent at 10 mM glucose and reversed by the combination of glucose plus AA compared to controls (**Fig. 6c**). While counterintuitive at first glance, this reversal was expected because of the restored glycolytic PEP supply and the ability of PCK2-deficient β-cells to generate a dysfunctional but sustained Ca^{2+} plateau fraction (**Fig. 3i**). Like the PCK2-βKO, in AA-stimulated islets from PKm1-βKO islets the Ca^{2+} and secretory responses were blunted at low glucose (**Fig. 6d,e**), whereas the insulin secretory response remained intact with glucose (**Fig. 6f**). These findings are entirely consistent with the differential nutrient response of PKm1-dependent Ca^{2+} and K_{ATP} channel closure described above (**Figs. 3 and 5**). The AA secretory response of PKm1-βKO islets was rescued by the presence of glucose (**Fig. 6f**), befitting the recruitment of PKm2 by glycolytic FBP.

Activated PKm2 has complementary functions during $Mito_{Cat}$ and $Mito_{Ox}$ accelerating both K_{ATP} closure and reopening, and consequently, AA-stimulated Ca^{2+} influx and extrusion (**Fig. 5**). Both the AA-induced Ca^{2+} response and insulin secretion were greatly increased in PKm2-βKO islets compared to controls (**Fig. 6g,h**). Glucose alone, but especially in combination with AA, stimulated enhanced secretion in the absence of PKm2 (**Fig. 6i**). While PKm1 is therefore sufficient to initiate secretion during $Mito_{Cat}$, PKm2 is essential for mitochondrial PEP to switch the system off during $Mito_{Ox}$. Thus, when PKm2 is replaced by the constitutively-activated PKm1,

the system is shifted towards greater nutrient-induced and, in particular PCK2-dependent, insulin secretion with heightened sensitivity to anaplerotic fuels.

DISCUSSION

These data provide evidence that PEP has metabolic control over PK-dependent ATP/ADP generation, K_{ATP} closure, Ca^{2+} signaling, and insulin secretion via the PEP cycle. β-cell deletions of PKm1, PKm2, and PCK2 provide a rigorous genetic validation of our hypothesized $Mito_{Cat}$-$Mito_{Ox}$ model of oscillatory metabolism, in which PK is controlled by two sources of PEP – glycolytic and mitochondrial (**Fig. 1a**). During the triggering phase, $Mito_{Cat}$, carbon from either carbohydrate or mitochondrial amino acid metabolism funnels through PCK2 to provide cataplerotic PEP to raise the ATP/ADP ratio in the K_{ATP} channel microcompartment. We show that both PK isoforms are present in the K_{ATP} microenvironment where they exert shared functional control of plasma membrane K_{ATP} closure via PEP hydrolysis. Mitochondrial PEP, generated by PCK2, was further linked to the ability of PKm2 to function as an "off-switch" during $Mito_{Ox}$, when K_{ATP} is reactivated and Ca^{2+} reduced to reset the oscillatory system. Although there is a large excess of PK enzyme, relative nutrient responses were used to elucidate how each PK isoform differentially participates in insulin secretion. Shifting from PKm2 to the PKm1 isoform was found to increase β-cell sensitivity to anaplerotic fuels.

In the mouse β-cell, we demonstrate that most of the PK is the constitutively-active PKm1 isoform, with a minor contribution from PKm2 and no detectable PKL activity. In the rat, MacDonald and Chang[12] reported PK activity to be primarily PKm2, which may be a species difference and/or an overestimation of the FBP responsivity which was modest. Our prior studies of PK-dependent K_{ATP} closure in human β-cell plasma membranes were conducted in the absence of FBP, which is consistent with the presence of PKm1 in the microdomain but not ruling out PKm2[1]. Regardless, PKm2 activators amplify nutrient-stimulated insulin secretion in mouse, rat, and human islets *in vitro*, and in rats *in vivo*, indicating that PKm2 is functionally recruitable in all three species[1,7].

Why are there two PK isoforms and how is it possible for PKm2 to contribute meaningfully, even when activated by FBP, given the abundance of PKm1 in mouse β-cells? Presently, we showed that defective K_{ATP} closure in PKm1-deficient β-cells can be rescued by PKm2 activation in excised patches and intact β-cells. Shared control of the K_{ATP} channel microcompartment may partly explain why the PKm1- and PKm2-βKO mice maintain normal glucose tolerance. In fact, a quantitative analysis of both first-phase and steady-state Ca^{2+} oscillations indicates that these isoforms are redundant at high glucose, conferring robustness to the system. Amino acids, as anaplerotic mitochondrial fuels, can generate mitochondrial PEP but do not elevate FBP by themselves. As such, at low glucose, anaplerotic fuels can only augment K_{ATP} closure via constitutively-active PKm1 or allosterically-activated (but not native) PKm2, which helps explain how shifting from PKm2 to PKm1 increases amino acid sensitivity. Combining both nutrients additionally recruits PKm2 as a coincidence signal to turn the system on more strongly, but also produces a stronger signal to switch the system off. From the

PCK2-βKO we learned that this off-signal is mitochondrial PEP, which is rate-limiting for cytosolic ATP/ADP and required to efficiently repolarize the β-cell. The PKm2 isozyme may respond to FBP by generating additional PCK2-derived PEP, explaining the associated failures of this off-switch and hypersecretion in the PKm2 and PCK2 deletion models when both glucose and amino acids are elevated.

Insulin release is frequently described in terms of triggering and amplifying on-switches termed "metabolic coupling factors" (MCFs). As defined by Prentki, "regulatory MCFs" are nutrient-dependent signals that facilitate the switch between metabolic networks (e.g. malonyl-CoA switches β-cells from fatty acid to glucose oxidation), while "effectory MCFs" (e.g., Ca^{2+}, ATP/ADP, monoacylglycerol, and reactive oxygen species), are transient, necessary, and sufficient on-signals that dose-dependently stimulate insulin secretion[2]. In that sense, is PEP a regulatory or effectory signal for insulin secretion – or both? PEP has some properties of a regulatory signal, since its metabolism by PK generates a bioenergetic feed forward that progressively deprives mitochondria of ADP, shutting down oxidative phosphorylation in favor of activating both pyruvate carboxylase and the PEP cycle[1,26]. Through a positive Hill coefficient, as the PEP concentration rises, it also progressively activates PKm2 to make more ATP[1,15], further reinforcing the PEP cycle. Arguably, PEP also has effectory properties, since its presence in the K_{ATP} microenvironment in the excised patches can override channel opening by continuous ADP to close K_{ATP} channels. This property requires either PKm1 or allosterically-activated PKm2. Likewise, in intact cells exposed to amino acids, PCK2-derived PEP was rate limiting to lower K_{ATP} conductance through a process independent of the bulk cytosolic ATP/ADP ratio. The ATP/ADP ratio at the plasma membrane is clearly effectory in that it is sufficient to cause depolarization[27–29] while at the same time priming granule exocytosis[30–32]. Assigning PEP an effectory role based on its essentiality and sufficiency would nevertheless be hasty as we do not yet know whether it dose-dependently increases exocytosis.

Effectory MCFs must be counterbalanced by a strong off-switch that ensures the signal is transient. That is, the β-cell would fail if K_{ATP}-dependent Ca^{2+} influx was activated without a coordinated homeostatic mechanism to turn it off. While glucose-dependent PKm2 activation during $Mito_{Cat}$ was found to facilitate K_{ATP} closure and increase Ca^{2+}, we also found during $Mito_{Ox}$ that PKm2 is essential for switching off Ca^{2+} and insulin secretion. Mechanistically, this off-switch was stimulated by allosteric PKm2 activation and ultimately facilitated K_{ATP} channel reopening in the intact β-cell, although most likely this effect is indirect. Where are the PK dependent off-switches if not in the plasma membrane microcompartment? In addition to compartmentalized K_{ATP} regulation, the $Mito_{Cat}$-$Mito_{Ox}$ model also invokes mitochondrial ADP privation as a control function of PK that limits $Mito_{Ox}$ (**Fig. S1**). This is based on the ability of PEP to locally control mitochondrial respiration in the presence of excess ADP[1,26]. Another important clue may be that impairing PEP cataplerosis, via β-cell PCK2 deletion, stalls the system in the Ca^{2+}-activated state and increases insulin secretion when anaplerosis is fully primed with glucose and amino acids. Stimulus-dependent movement of the mitochondria away from the plasma membrane[25] may also be important for mitochondrial PEP to switch the system on and off. Further studies are needed to

elucidate the understudied homeostatic functions of PKm2 and mitochondrial PEP, and may help to explain how overnutrition perturbs β-cell function in diabetes.

ACKNOWLEDGEMENTS

We would like to thank Matthew Vander Heiden (MIT) for providing PKm1$^{f/f}$ mice, and Mark Huising (UC-Davis) and Barak Blum (UW-Madison) for providing Ucn3-Cre mice. We would also like to acknowledge Kathy Krentz and Dustin Rubenstein at the UW-Madison Genome Editing and Animal Model Core for their assistance generating PCK2$^{f/f}$ mice, and Jiwon Seo and Jody Peter at the UW-Madison Biomedical Research Model Services Breeding Core for their assistance with animal husbandry and genotyping. The Merrins laboratory gratefully acknowledges support from the NIH/NIDDK (R01DK113103 and R01DK127637) and the Department of Veterans Affairs (I01B005113). HRF received a postdoctoral fellowships from HRSA (T32HP10010) and the NIH/NIA (T32AG000213), SLL received a predoctoral fellowship from the NIH/NIDDK (T32DK007665), HRV received a postdoctoral fellowship from the American Diabetes Association (1-17-PDF-155), and we acknowledge Dudley Lamming for contributing support for EP from R01AG062328. The Kibbey laboratory gratefully acknowledges support from the NIH/NIDDK (R01DK127637). This work utilized facilities and resources from the William S. Middleton Memorial Veterans Hospital and does not represent the views of the Department of Veterans Affairs or the United States Government.

AUTHOR CONTRIBUTIONS

MJM conceived the study and wrote the paper with HRF and RGK. HRF performed the main body of the experiments with assistance from TH, EP, SMS, SLL, HRV, SMD, and RLC. MJM and RGK provided resources. All authors interpreted the data and edited the manuscript.

DECLARATION OF INTERESTS

The authors declare no competing interests.

MATERIALS AND METHODS

Mice Creation

β-cell specific PKm1 and PKm2 knockout mice were generated by breeding *Ins1-Cre*[17] mice (B6(Cg)-*Ins1*$^{tm1.1(cre)Thor}$/J, Jackson Laboratory #026801) with *Pkm1*$^{f/f}$ mice[14,18] provided by Matthew Vander Heiden (MIT) or *Pkm2*$^{f/f}$ mice[19] (B6;129S-*Pkm*$^{tm1.1Mgvh}$/J, Jackson Laboratory #024408) after 10 generations of backcrossing to C57BL6/J mice (Jackson Laboratory). *Pck2*$^{f/f}$ mice were generated *de novo* by the University of Wisconsin-Madison Genome Editing and Animal Model core. Backcrossed F1s were sequence confirmed by Illumina targeted deep sequencing to confirm the LoxP insertions around exon 5 (ENSMUSE00000399990; **Fig. S1**), and the intervening region was sequence confirmed with Sanger sequencing. *Pck2*$^{f/f}$ mice were crossed with *Ucn3-Cre* mice[20] provided by Barak Blum (University of Wisconsin-Madison) with

permission from Mark O. Huising (University of California-Davis). All mice were genotyped by Transnetyx.

Mouse Islet Preparations

Male mice were housed 2-5 per cage at 21-23°C, fed with a chow diet and water provided *ad libitum*, and maintained on a 12 h light/dark cycle. Mice 12-20 weeks of age were sacrificed via CO_2 asphyxiation followed by cervical dislocation, and islets were isolated using methods previously described[22].

Cloning and Adenoviral Delivery of Biosensors

Generation of adenovirus carrying genetically-encoded ATP/ADP biosensors (Perceval-HR) under control of the insulin promoter was described previously[16]. High-titer adenovirus was added to islets immediately after islet isolation and incubated for 2 h at 37°C then moved to fresh media. Imaging was performed 3 days post isolation.

Western blots

Islets were lysed using 0.1% Triton-X100 in phosphate buffered saline (1 µl/islet). Islets in lysis buffer were incubated at room temperature for 15 minutes, vortexed for 30 seconds, frozen/thawed, and vortexed for 30 seconds again. Cell lysate was spun down at max speed in a table top centrifuge and 16-20 µl supernatant was added to each well of a 12% SDS-PAGE gel. The gel was run at 110V for ~2 hours then transferred to a PVDF membrane at 100V for 1 hour at 4°C. Membranes were blocked in 4% BSA in Tris-buffered saline containing 0.1% Tween-20 detergent (TBST) for 30 minutes then incubated overnight with PKm1 (Cell Signaling #4053; 1:1000), PKm2 (Cell Signaling #7067; 1:1000), PCK2 primary antibodies (Cell Signaling #6924; 1:1000), or loading controls beta-actin (Cell Signaling #3700; 1:1000) or HSP90 (Cell Signaling #4877; 1:1000). Blots were washed for 15 min in TBST four times then incubated for 2 hours at room temperature with an anti-rabbit IgG HRP-linked secondary antibody (Cell Signaling #7074; 1:20,000). Blots were imaged and quantified using ImageQuant (Amersham).

Timelapse Imaging

Islets were preincubated in 2.5 µM FuraRed (Molecular Probes F3020) in RPMI 1640 for 45 minutes at 37°C prior to being placed in an glass-bottomed imaging chamber (Warner Instruments) on a Nikon Eclipse Ti-E inverted microscope with a Super Flour 10x/0.5N.A. objective (Nikon Instruments). The chamber was perfused with standard imaging solution (in mM: 135 NaCl, 4.8 KCl, 5 $CaCl_2$, 20 HEPES, 1.2 $MgCl_2$) for low glucose/amino acid experiments, or HBSS (in mM 137 NaCl, 5.6 KCl, 1.2 $MgCl_2$, 0.5 NaH_2PO_4, 4.2 $NaHCO_3$, 10 HEPES, 2.6 $CaCl_2$) for high glucose experiments containing glucose and amino acid concentrations indicated in figure legends. Temperature was maintained at 33°C with inline solution and chamber heaters (Warner Instruments), and flow rate was set to 0.25 ml/min. Excitation was provided by a SOLA SE II 365 (Lumencor). A Hamamatsu ORCA-Flash4.0 V2 Digital CMOS camera was used to collect

fluorescence emission at 0.125-0.2 Hz. Nikon NIS-Elements was used to designate regions of interest. Excitation (x) and emission (m) filters (ET type; Chroma Technology) were used with an FF444/521/608-Di01 dichroic (Semrock) as follows: FuraRed, 430/20x and 500/20x, 630/70m (R430/500 was reported) and Perceval-HR, 430/20x and 500/20x, 535/35m (R500/430 was reported). A custom MATLAB script was used to quantify cytosolic Ca^{2+} oscillation parameters. In order to differentiate between islets of control and knockout mice, islets of one genotype were barcoded by pre-incubation with 2 µM DiR (Fisher Scientific D12731) or 2 µM DiD (Fisher Scientific D7757) in islet media for 10 minutes at 37°C. Islet barcodes were then imaged using a Cy7 (for DiR) or Cy5 filter cube (for DiD) from Chroma.

Electrophysiology

Single channel patch clamp experiments and data analysis were performed as previously described[1]. Briefly, mouse and human cells were acutely isolated by dispersing of islets with Accutase (Fisher Scientific). Cells were plated on sterilized uncoated glass shards and kept at 37ºC with 95% O_2-5% CO_2. For both on-cell and inside-out recordings, gigaseals were obtained in extracellular bath solution (in mM): 140 NaCl, 5 KCl, 1.2 $MgCl_2$, 2.5 $CaCl_2$, 0.5 Glucose, 10 HEPES, pH 7.4, adjusted with NaOH and clamped at −50mV. For inside-out configuration, after pipette excision, the bath solution was replaced with equilibrium solutions with K^+ as the charge carrier (in mM): 130 KCl, 2 $CaCl_2$, 10 EGTA, 0.9 $[Mg^{2+}]_{free}$, 10 sucrose, 20 HEPES, pH 7.2 with KOH. The $[Mg^{2+}]_{free}$, calculated using WEBMAXC standard, was held constant in the presence of nucleotides. The pipette solution, used for both on-cell and inside-out configurations, contained (in mM): 10 sucrose, 130 KCl, 2 $CaCl_2$, 10 EGTA, 20 HEPES, pH 7.2, adjusted with KOH. Recording electrodes made of microfilament borosilicate glass (Harvard Apparatus, Holliston, MA #64-0792) were used to pull patch pipettes (3 MΩ) on a horizontal Flaming/Brown micropipette puller (P-1000, Sutter Instruments) and polished by microforge (Narishige MF-830) to a final tip resistance of 5-10 MΩ. On-cell recording started after formation of a stable gigaseal (>2.5 GΩ) and inside-out recording started after withdrawal of the pipette and establishment of the excised inside-out configuration. A HEKA Instruments EPC10 patch-clamp amplifier was used for registration of current. Data was Bessel filtered online at 1 kHz and single channel currents were analyzed offline using ClampFit analysis module of pCLAMP 10 software (Molecular Devices).

Islet Perifusion Assays

Islets from 6 mice of each genotype were pooled and then divided in equal numbers and placed into a 12-channel perifusion system (BioRep Peri-4.2; 75-100 islets/chamber) containing KRPH buffer (in mM: 140 NaCl, 4.7 KCl, 1.5 $CaCl_2$, 1 NaH_2PO_4, 1 $MgSO_4$, 2 $NaHCO_3$, 5 HEPES, 2 glucose, 0.1% fatty acid-free BSA, pH 7.4) with 100 µl Bio-Gel P-4 Media (Bio-Rad). Islets were equilibrated at 2 mM glucose for 36-48 minutes prior to perfusion with amino acids or 10 mM glucose at 37ºC. Insulin secretion was assayed using Promega Lumit™ Insulin Immunoassay (CS3037A01) and measured using a TECAN Spark plate reader. Quant-IT PicoGreen dsDNA

Assay Kit (Thermo Scientific P7589) was used to determine DNA content after lysis using 0.1% Triton X-100.

PK activity

The enzymatic activity of pyruvate kinase was measured using EC 2.7.1.40 from Sigma[33] as described previously[1]. FBP (Sigma Aldrich #F6803) and TEPP-46 (PKa; Fisher Scientific #50-548-70001) were used at a concentration of 80 µM and 10 µM, respectively. Experiments were performed at 37ºC.

Quantification and Statistical Analysis

Figure legends describe the statistical details of each experiments. Data are expressed as mean ± SEM. Statistical significance was determined by two-way or one-way ANOVA with Sidak multiple-comparisons test post hoc or Student's t-test as indicated in the figure legends. Data were continuous and normally distributed so were analyzed with parametric tests. Differences were considered to be significant at $P < 0.05$. Calculations were performed using GraphPad Prism.

REFERENCES

1. Lewandowski, S. L. *et al.* Pyruvate Kinase Controls Signal Strength in the Insulin Secretory Pathway. *Cell Metab* **32**, 736-750.e5 (2020).
2. Prentki, M., Matschinsky, F. M. & Madiraju, S. R. M. Metabolic signaling in fuel-induced insulin secretion. *Cell Metab.* **18**, 162–185 (2013).
3. Thompson, B. & Satin, L. S. Beta-Cell Ion Channels and Their Role in Regulating Insulin Secretion. *Compr Physiol* **11**, 1–21 (2021).
4. Campbell, J. E. & Newgard, C. B. Mechanisms controlling pancreatic islet cell function in insulin secretion. *Nat Rev Mol Cell Biol* **22**, 142–158 (2021).
5. Corkey, B. E. Targeting Pyruvate Kinase PEPs Up Insulin Secretion and Improves Glucose Homeostasis. *Cell Metab* **32**, 693–694 (2020).
6. Nicholls, D. G. The Pancreatic β-Cell: A Bioenergetic Perspective. *Physiol. Rev.* **96**, 1385–1447 (2016).
7. Abulizi, A. *et al.* Multi-Tissue Acceleration of the Mitochondrial Phosphoenolpyruvate Cycle Improves Whole-Body Metabolic Health. *Cell Metab* **32**, 751-766.e11 (2020).
8. Stark, R. *et al.* Phosphoenolpyruvate cycling via mitochondrial phosphoenolpyruvate carboxykinase links anaplerosis and mitochondrial GTP with insulin secretion. *J. Biol. Chem.* **284**, 26578–26590 (2009).
9. Jesinkey, S. R. *et al.* Mitochondrial GTP Links Nutrient Sensing to β Cell Health, Mitochondrial Morphology, and Insulin Secretion Independent of OxPhos. *Cell Rep* **28**, 759-772.e10 (2019).
10. DiGruccio, M. R. *et al.* Comprehensive alpha, beta and delta cell transcriptomes reveal that ghrelin selectively activates delta cells and promotes somatostatin release from pancreatic islets. *Mol Metab* **5**, 449–458 (2016).

11. Mitok, K. A. *et al.* Islet proteomics reveals genetic variation in dopamine production resulting in altered insulin secretion. *J. Biol. Chem.* **293**, 5860–5877 (2018).
12. MacDonald, M. J. & Chang, C. M. Pancreatic islets contain the M2 isoenzyme of pyruvate kinase. Its phosphorylation has no effect on enzyme activity. *Mol. Cell. Biochem.* **68**, 115–120 (1985).
13. Anastasiou, D. *et al.* Pyruvate kinase M2 activators promote tetramer formation and suppress tumorigenesis. *Nat. Chem. Biol.* **8**, 839–847 (2012).
14. Li, Q. *et al.* PKM1 Exerts Critical Roles in Cardiac Remodeling Under Pressure Overload in the Heart. *Circulation* **144**, 712–727 (2021).
15. Merrins, M. J., Van Dyke, A. R., Mapp, A. K., Rizzo, M. A. & Satin, L. S. Direct measurements of oscillatory glycolysis in pancreatic islet β-cells using novel fluorescence resonance energy transfer (FRET) biosensors for pyruvate kinase M2 activity. *J. Biol. Chem.* **288**, 33312–33322 (2013).
16. Merrins, M. J. *et al.* Phase Analysis of Metabolic Oscillations and Membrane Potential in Pancreatic Islet β-Cells. *Biophys. J.* **110**, 691–699 (2016).
17. Thorens, B. *et al.* Ins1(Cre) knock-in mice for beta cell-specific gene recombination. *Diabetologia* **58**, 558–565 (2015).
18. Davidson, S. M. *et al.* Pyruvate kinase M1 suppresses development and progression of prostate adenocarcinoma. 2021.05.09.443334 (2021) doi:10.1101/2021.05.09.443334.
19. Israelsen, W. J. *et al.* PKM2 isoform-specific deletion reveals a differential requirement for pyruvate kinase in tumor cells. *Cell* **155**, 397–409 (2013).
20. van der Meulen, T. *et al.* Virgin Beta Cells Persist throughout Life at a Neogenic Niche within Pancreatic Islets. *Cell Metab.* **25**, 911-926.e6 (2017).
21. Kibbey, R. G. *et al.* Mitochondrial GTP insensitivity contributes to hypoglycemia in hyperinsulinemia hyperammonemia by inhibiting glucagon release. *Diabetes* **63**, 4218–4229 (2014).
22. Gregg, T. *et al.* Pancreatic β-Cells From Mice Offset Age-Associated Mitochondrial Deficiency With Reduced KATP Channel Activity. *Diabetes* **65**, 2700–2710 (2016).
23. Gregg, T. *et al.* Obesity-dependent CDK1 signaling stimulates mitochondrial respiration at complex I in pancreatic β-cells. *J. Biol. Chem.* **294**, 4656–4666 (2019).
24. Kennedy, H. J. *et al.* Glucose generates sub-plasma membrane ATP microdomains in single islet beta-cells. Potential role for strategically located mitochondria. *J. Biol. Chem.* **274**, 13281–13291 (1999).
25. Griesche, N., Sanchez, G., Hermans, C. & Idevall-Hagren, O. Cortical mitochondria regulate insulin secretion by local Ca2+ buffering in rodent beta cells. *J Cell Sci* **132**, jcs228544 (2019).
26. Sugden, M. C. & Ashcroft, S. J. Phosphoenolpyruvate in rat pancreatic islets: a possible intracellular trigger of insulin release? *Diabetologia* **13**, 481–486 (1977).
27. Cook, D. L. & Hales, C. N. Intracellular ATP directly blocks K+ channels in pancreatic B-cells. *Nature* **311**, 271–273 (1984).

28. Ashcroft, F. M., Harrison, D. E. & Ashcroft, S. J. Glucose induces closure of single potassium channels in isolated rat pancreatic beta-cells. *Nature* **312**, 446–448 (1984).
29. Rorsman, P. & Trube, G. Glucose dependent K+-channels in pancreatic beta-cells are regulated by intracellular ATP. *Pflugers Arch.* **405**, 305–309 (1985).
30. Eliasson, L., Renström, E., Ding, W. G., Proks, P. & Rorsman, P. Rapid ATP-dependent priming of secretory granules precedes Ca(2+)-induced exocytosis in mouse pancreatic B-cells. *J. Physiol. (Lond.)* **503 (Pt 2)**, 399–412 (1997).
31. Takahashi, N. *et al.* Post-priming actions of ATP on Ca2+-dependent exocytosis in pancreatic beta cells. *Proc. Natl. Acad. Sci. U.S.A.* **96**, 760–765 (1999).
32. Pizarro-Delgado, J., Deeney, J. T., Corkey, B. E. & Tamarit-Rodriguez, J. Direct Stimulation of Islet Insulin Secretion by Glycolytic and Mitochondrial Metabolites in KCl-Depolarized Islets. *PLoS ONE* **11**, e0166111 (2016).
33. Bergmeyer, H.U., Gawehn, K., & Grassl, M. Methods of Enzymatic Analysis. in vol. I 5109–510 (Academic Press, Inc.).

Figure 1

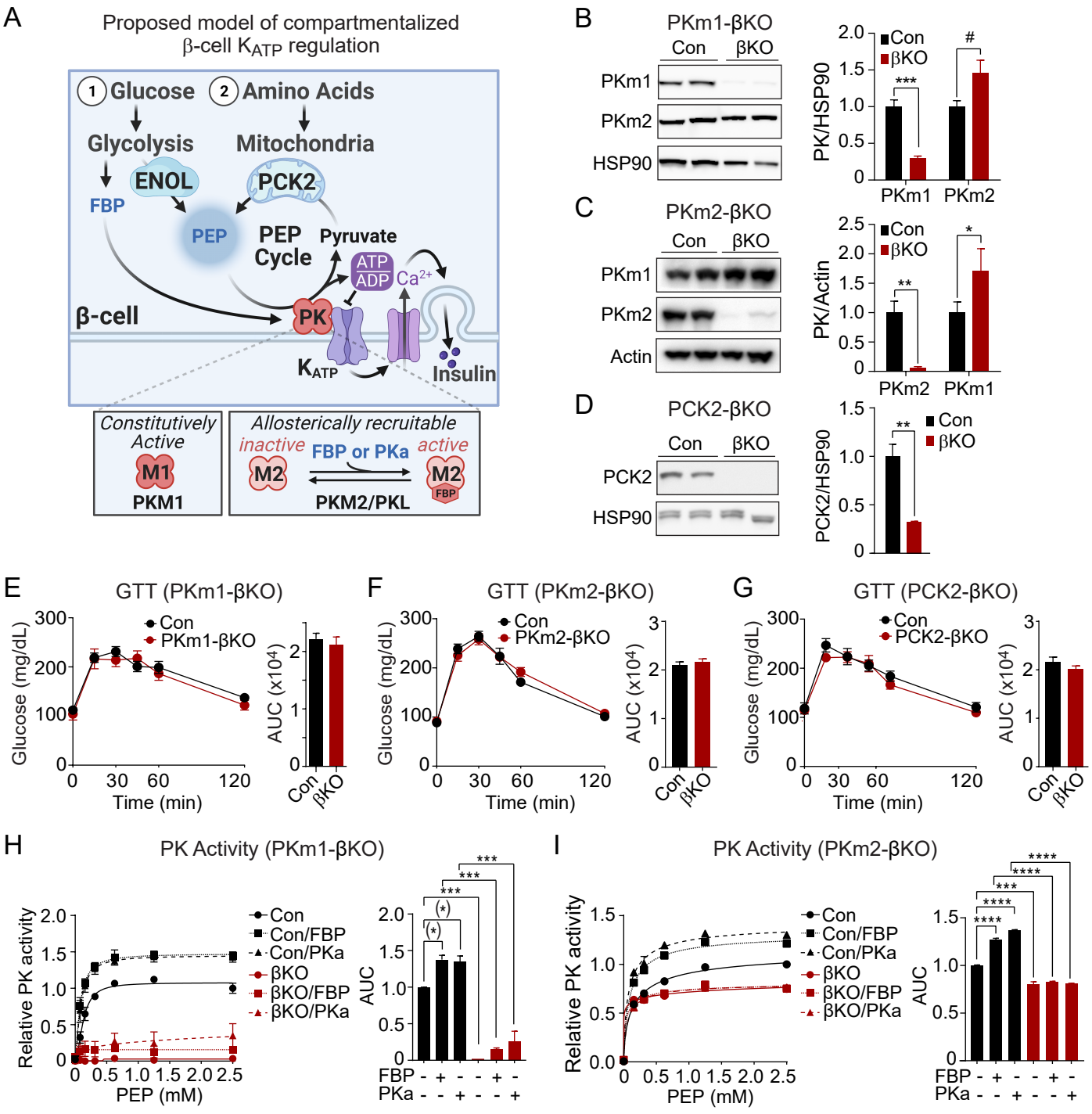

Figure 1. Generation of mouse models to probe the functions of PKm1, PKm2, and PCK2 in β-cells.

(A) Hypothesized model in which PK in the K_{ATP} microcompartment is fueled by two sources of PEP—glycolytic PEP generated by enolase, and mitochondrial PEP generated by PCK2 in response to anaplerotic fuels. β-cells express three isoforms of PK, constitutively active PKm1 and allosterically recruitable PKm2 and PKL that are activated by endogenous fructose 1,6-bisphosphate (FBP) or pharmacologic PK activators (PKa).

(B-D) Quantification of knockdown efficiency in islet lysates from PKm1-βKO (B), PKm2-βKO (C), and Pck2-βKO mice (D) (n = 4 mice).

(E-G) Intraperitoneal glucose tolerance tests (GTT, 1 g/kg) of PKm1-βKO mice (n = 9) and littermate controls (n = 8) (E), PKm2-βKO mice (n = 7) and littermate controls (n = 7) (F), and Pck2-βKO mice (n = 10) and littermate controls (n = 7) (G) following an overnight fast.

(H-I) PK activity in islet lysates of PKm1-βKO (H) and PKm2-βKO mice (I) in response to FBP (80 μM) and PKa (10 μM TEPP-46). (n = 2 replicates from 6 mice/group)

Data are shown as mean ± SEM. $^{\#}P < 0.01$, $^{*}P < 0.05$, $^{**}P < 0.01$, $^{***}P < 0.001$, $^{****}P < 0.0001$ by t-test (B-G) or two-way ANOVA (H-I).

Figure 2

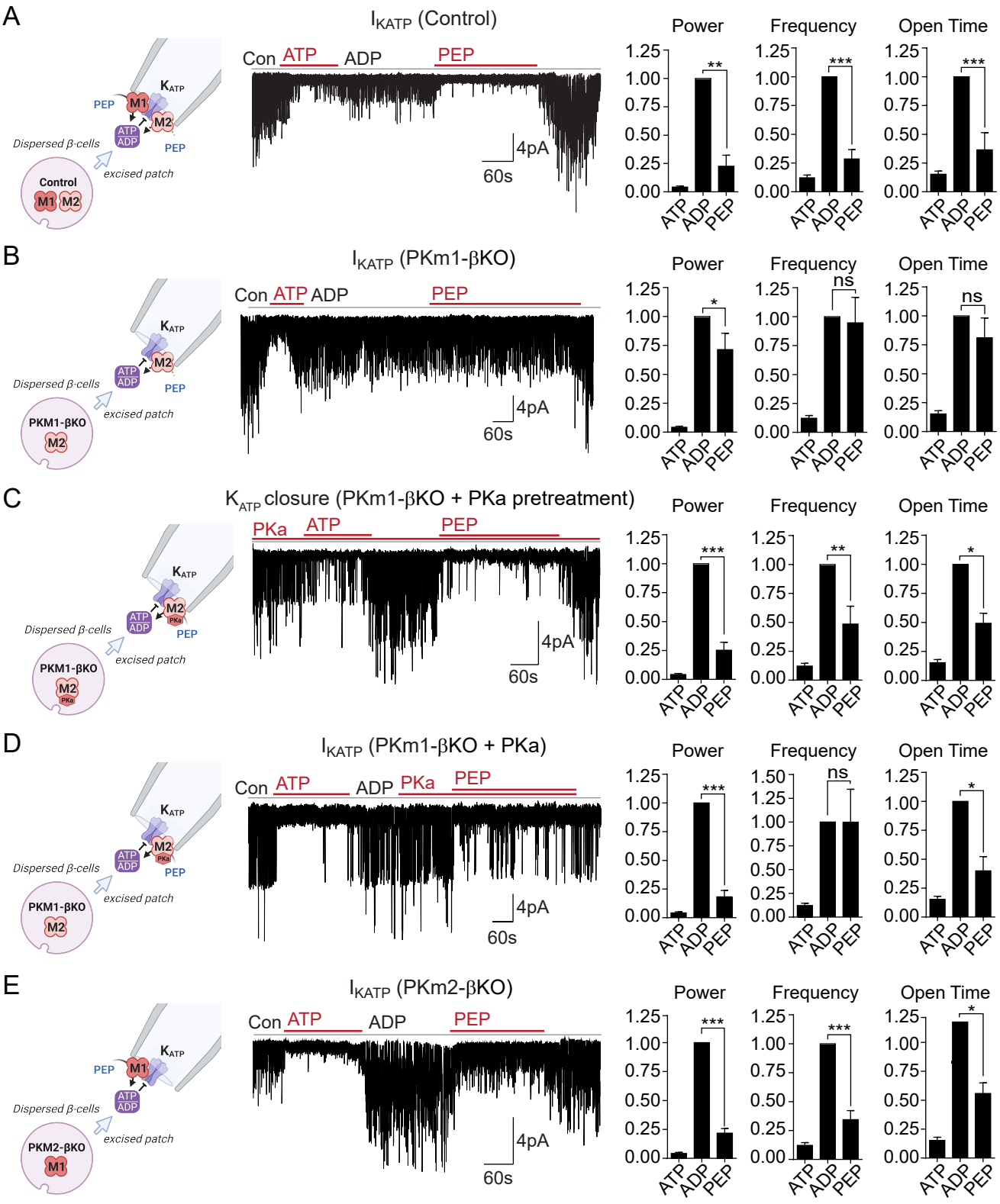

Figure 2. Plasma membrane K_{ATP} channels are locally regulated by a combination of PKm1 and allosterically activated PKm2.

(A-E) K_{ATP} channel activity (holding potential = -50 mV) quantified in terms of power, frequency, and open time. Applying the substrates for PK closes K_{ATP} channels in excised patches of β-cell plasma membrane from control mice (n = 14 recordings from 4 mice) (A). Defective K_{ATP} channel closure in β-cells from PKm1-KO (n = 20 recordings from 5 mice) (B) is rescued by PKa pretreatment (n = 6 recordings from 3 mice) (C) and acute PKa application (n = 7 recordings from 3 mice) (D). PKm1 is sufficient for K_{ATP} closure in β-cells from PKm2-βKO (n = 6 recordings from 3 mice) (E). ATP, 1 mM; ADP, 0.5 mM ADP + 0.1 mM ATP; PEP, 5 mM; PKa, 10 μM TEPP-46.

Data are shown as mean ± SEM. *P < 0.05, **P < 0.01, ***P < 0.001, **** P < 0.0001 by paired t-test. $^{(*)}P$ < 0.05 by unpaired t-test in (H).

Figure 3

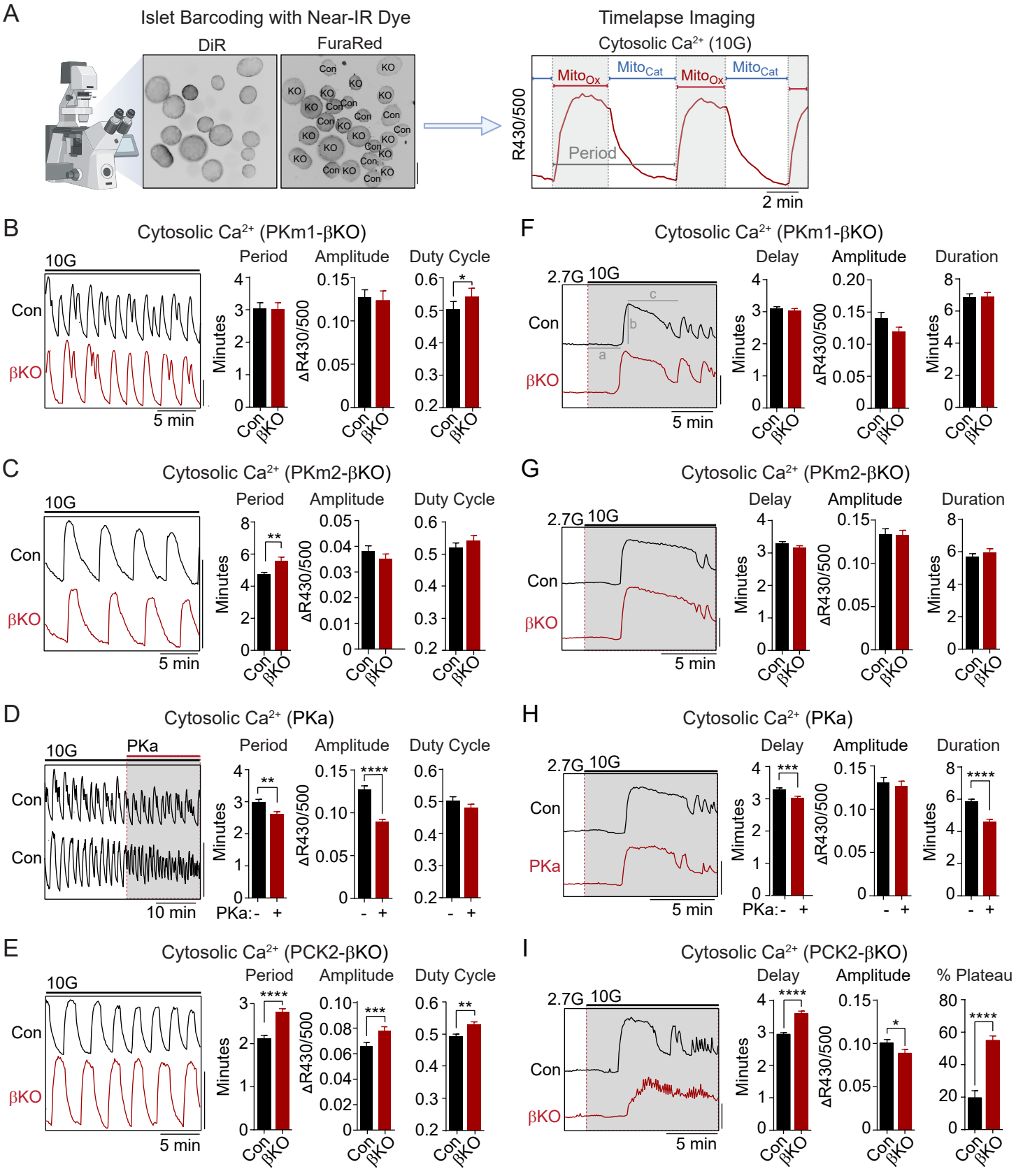

Figure 3. PKm2 and PCK2, but not PKm1, have metabolic control over first-phase and steady-state Ca^{2+} influx in response to glucose.

(A) Barcoding of islet preparations with near-IR dye (DiR) permits simultaneous timelapse imaging of islet Ca^{2+} dynamics of control and βKO mice (scale bar = 200 μm) (*left*). A representative trace illustrates the cataplerotic triggering phase ($Mito_{Cat}$) and oxidative secretory phases ($Mito_{Ox}$) of steady-state Ca^{2+} oscillations in the presence of 10 mM glucose and 1 mM leucine (*right*). Gray line denotes the period.

(B-E) Representative traces and quantification of period, amplitude, and duty cycle of steady-state Ca^{2+} oscillations in islets from PKm1-βKO (*n* = 91 islets from 3 mice) and littermate controls (*n* = 94 islets from 3 mice) (B), PKm2-βKO (*n* = 118 islets from 4 mice) and littermate controls (*n* = 111 islets from 4 mice) (C), control mice treated with PKa (10 μM TEPP-46) (*n* = 88 islets from 3 mice), and PCK2-βKO (*n* = 74 islets from 3 mice) and littermate controls (*n* = 77 islets from 3 mice) (E). The bath solution (PSS) contained 10 mM glucose (10G) and 1 mM leucine. Scale bars: 0.1 FuraRed excitation ratio (R430/500).

(F-I) Representative Ca^{2+} traces and quantification of time to depolarization (a), first-phase amplitude (b), and first-phase duration (c) in islets from PKm1-βKO (*n* = 144 islets from 6 mice) and littermate controls (*n* = 150 islets from 6 mice) (B), PKm2-βKO (*n* = 52 islets from 2 mice) and littermate controls (*n* = 55 islets from 2 mice) (C), PKa-treated (10 μM TEPP-46) (*n* = 161 islets from 9 mice) and vehicle controls (*n* = 212 islets from 9 mice), and PCK2-βKO (*n* = 73 islets from 3 mice) and littermate controls (*n* = 78 islets from 3 mice) (E). The bath solution (PSS) contained 1 mM leucine and 2.7 mM (2.7G) and 10 mM glucose (10G) as indicated. Scale bars: 0.1 FuraRed excitation ratio (R430/500).

Data are shown as mean ± SEM. **P* < 0.05, ***P* < 0.01, ****P* < 0.001, **** *P* < 0.0001 by unpaired t-test (A-C and E-I) and paired t-test (D).

Figure 4

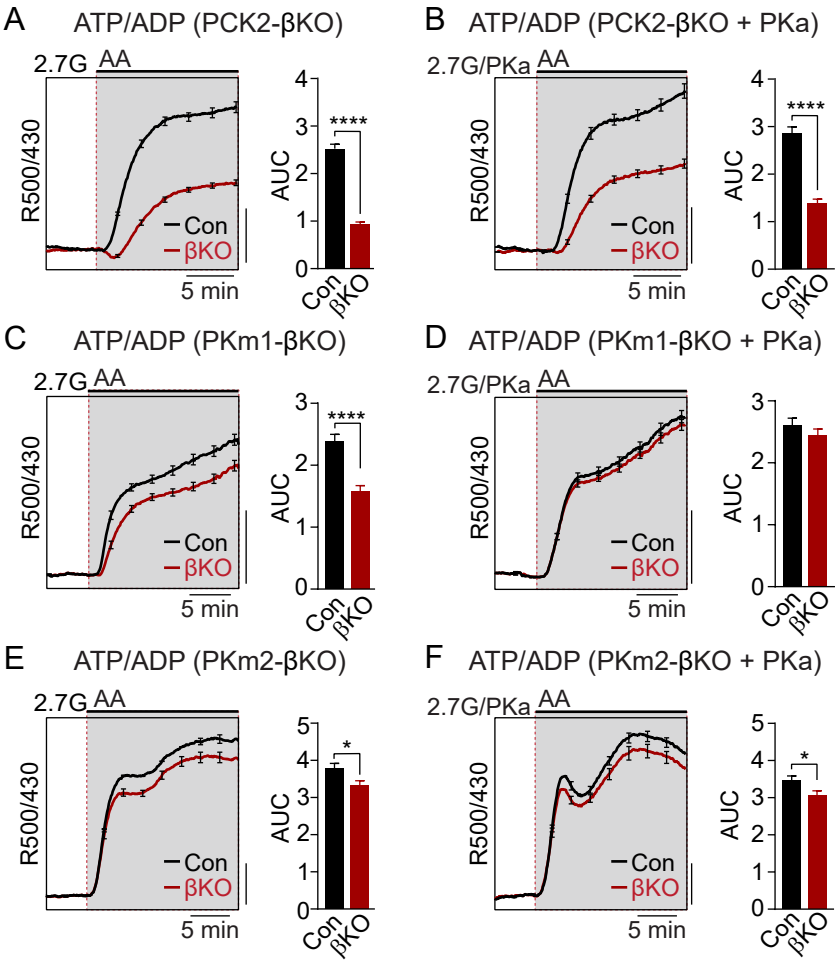

Figure 4. Restriction of the glycolytic PEP supply reveals the importance of PCK2 for cytosolic ATP/ADP.

Average β-cell ATP/ADP in islets from PCK2-βKO (A-B), PKm1-βKO (B-E), and PKm2-βKO (E-F) mice in response to mixed amino acids (AA) provided at three times their physiological concentrations (1x = Q, 0.6 mM; L, 0.5 mM; R, 0.2 mM; A, 2.1 mM) in the presence of 2.7 mM glucose (2.7G) to remove the enolase contribution to cytosolic PEP. PKa (10 μM TEPP-46) was present in B, D, and F. ATP/ADP is quantified as area under the curve (AUC) from PCK2-βKO (vehicle, n = 73 islets from 3 mice; PKa, n = 71 islets from 3 mice) and littermate controls (vehicle, n = 90 islets from 3 mice; PKa, n = 77 islets from 3 mice); PKm1-βKO (vehicle, n = 66 islets from 3 mice; PKa, n = 72 islets from 3 mice) and littermate controls (vehicle, n = 69 islets from 6 mice; PKa, n = 69 islets from 3 mice); and PKm2-βKO (vehicle, n = 99 islets from 3 mice; PKa, n = 89 islets from 3 mice) and littermate controls (vehicle, n = 100 islets from 6 mice; PKa, n = 85 islets from 3 mice). Scale bars: 0.1 Perceval-HR excitation ratio (R500/430).

Data are shown as mean ± SEM. *P < 0.05, **** P < 0.0001 by t-test.

Figure 5

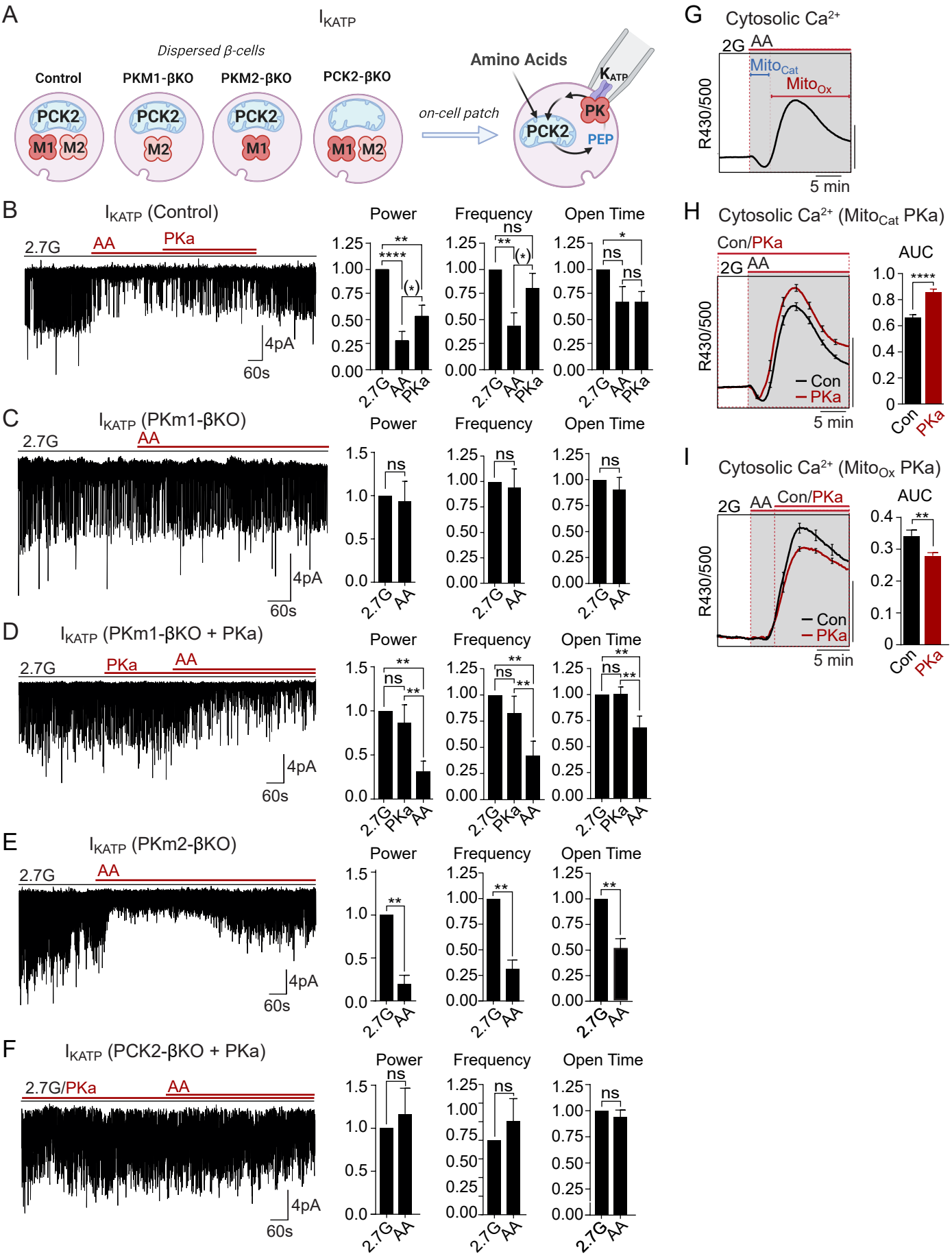

Figure 5. Mitochondrial PEP signals to PK within the plasma membrane K_{ATP} channel microcompartment in intact β-cells.

(A) Diagram of on-cell patch clamp method in intact β-cells with bath application of amino acids.

(B-F) Representative example traces and quantification of K_{ATP} channel closure in terms of normalized power, frequency, and open time for β-cells from control (n = 10 recordings from 3 mice) (A), PKm1-βKO (n = 7 recordings from 3 mice) (B-C), PKm2-βKO (n = 7 recordings from 3 mice) (E), and PCK2-βKO mice (n = 10 recordings from 3 mice) (F) in response to mixed amino acids (AA) and 2.7 glucose (2.7G) as in Fig. 4.

(G-I) AA-stimulated Ca^{2+} responses in control islets illustrating the $Mito_{Cat}$ and $Mito_{Ox}$ phases (A). The average Ca^{2+} response to PKa application during $Mito_{Cat}$ (vehicle, n =575 islets from 8 mice; PKa, n = 575 islets from 8 mice) (H) and $Mito_{Ox}$ (vehicle, n = 91 islets from 4 mice; PKa, n = 108 islets from 4 mice) (I) is quantified as AUC. Scale bars: 0.025 FuraRed excitation ratio (R430/500).

Data are shown as mean ± SEM. *P < 0.05, **P < 0.01, ***P < 0.001, **** P < 0.0001 by paired one-way ANOVA or paired t-test as appropriate. Following the removal of one outlier by ROUT (Q=10%), $^{(*)}P$ < 0.05 by paired t-test in (B).

Figure 6

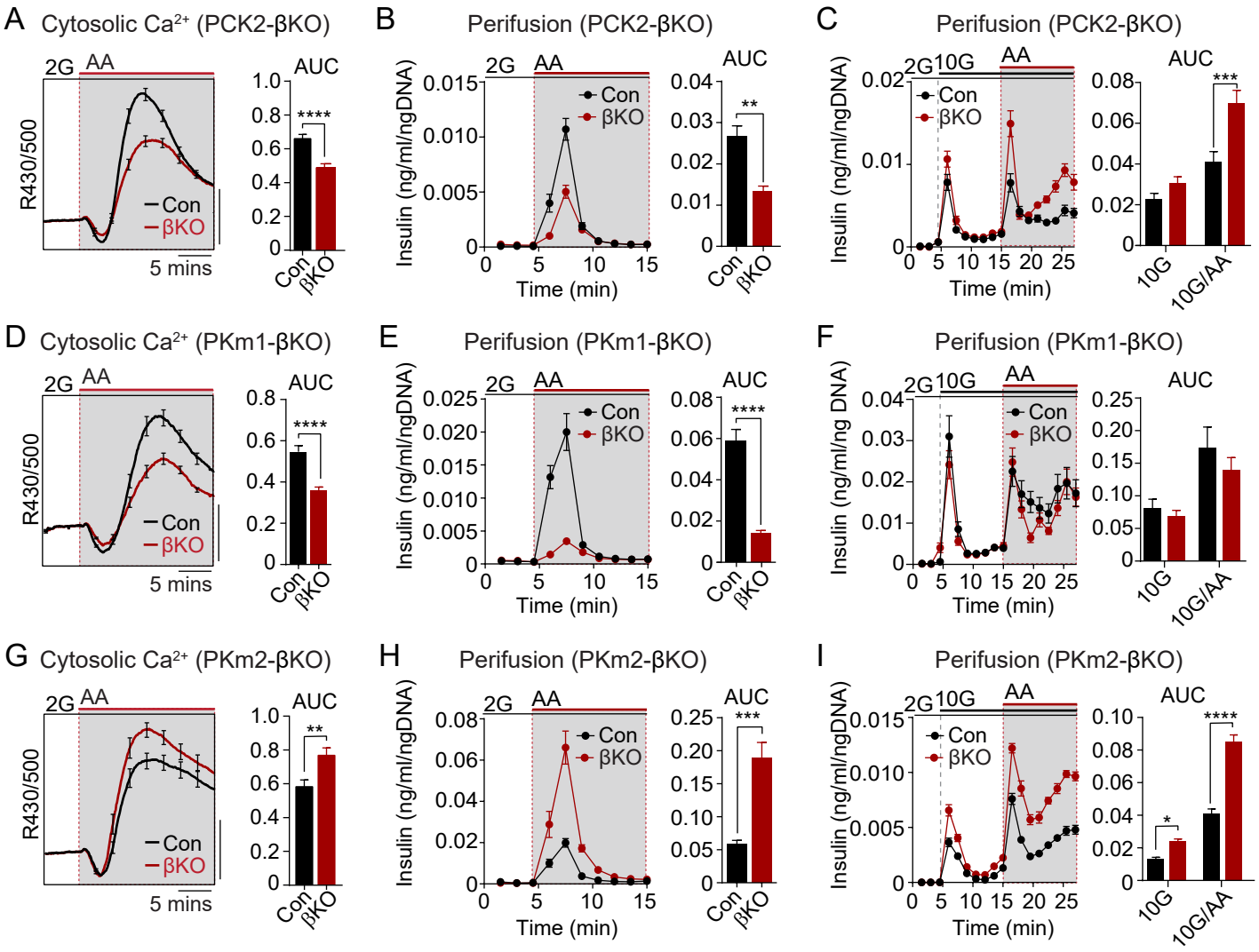

Figure 6. The PKm1/PKm2 ratio dictates the β-cell Ca^{2+} and secretory response to anaplerotic fuels.

Average cytosolic Ca^{2+} and insulin secretory responses in controls and PCK2-βKO (A-C), PKm1-βKO (D-F) and PKm2-βKO islets (G-I) to the indicated concentrations of glucose (2G, 2 mM; 10G, 10 mM) and amino acids (AA; concentrations are listed in Fig. 4). Data are quantified as AUC. Islet Ca^{2+} data reflect n = 60-101 islets from 3 mice per condition (scale bar = 0.025 FuraRed excitation ratio). Islet perifusion data reflect n = 100 islets per mouse and 6 mice per condition except PKm2-βKO at high glucose (5 mice).

Data are shown as mean ± SEM. *p<0.05, **p<0.01, ***p<0.001, ****p<0.0001 by t-test.